

Modelling the barotropic tides in the Strait of Sicily and Tunisian shelf

Numerical models
Tides
Harmonic constituents
Mediterranean
Strait of Sicily

Modèles numériques
Marées
Composantes harmoniques
Méditerranée
Déroit de Sicile

Jean-Marc MOLINES

Permanent affiliation: Software Based System, 13590 Meyreuil, France.
Institut de Mécanique de Grenoble, BP 53 X, 38041 Grenoble Cedex, France.

Received 30/07/90, in revised form 22/01/91, accepted 30/01/91.

ABSTRACT

In order to check the sea-level variability in the vicinity of Lampedusa Island (in the frame of Topex/Poseidon altimeter calibration), a numerical model of the tides for the Strait of Sicily and adjacent area has been performed. Cotidal and co-range charts for the main diurnal and semidiurnal constituents are drawn and the model results are compared with *in situ* data. Position of amphidromes for these constituents is also clarified: a strong semidiurnal resonance observed in the Gulf of Gabes is well reproduced in the model. Semidiurnal tidal currents are found to be important at the Adventure Bank (South-West of Sicily) and in the Gulf of Gabes. Diurnal tidal currents, dominant on Adventure Bank, are due to energy trapped around the Western extremity of Sicily, that probably generate the strong diurnal internal waves which are observed in this area.

Oceanologica Acta, 1991. **14**, 3, 241-252.

RÉSUMÉ

Modélisation des marées barotropes dans le détroit de Sicile et sur le plateau continental tunisien

Dans le but d'étudier la variabilité du niveau de la mer au voisinage de l'île de Lampedusa (dans le cadre de la calibration de l'altimètre de Topex/Poseidon), un modèle numérique de marée a été développé pour la zone du détroit de Sicile. Les principales composantes diurnes et semi-diurnes de la marée sont présentées sous forme de cartes cotidales et les résultats du modèle sont comparés aux observations existantes. La position des points amphidromiques pour ces composantes est précisée et la résonance des ondes semi-diurnes dans le Golfe de Gabès est bien reproduite. Les courants de marée associés aux ondes semi-diurnes sont importants sur le banc de l'Aventure (sud-ouest de la Sicile) et dans le Golfe de Gabès. Ceux associés aux ondes diurnes n'ont d'importance que sur le banc de l'Aventure où ils sont dominants et liés au piégeage de l'énergie diurne à l'extrémité ouest de la Sicile. Ils contribuent probablement à la génération des fortes ondes internes diurnes observées dans cette zone.

Oceanologica Acta, 1991. **14**, 3, 241-252.

INTRODUCTION

Lampedusa Island (located in the southern part of the Sicily Strait) was chosen as a possible candidate for the CNES calibration/validation site for the radar altimeters of Topex/Poseidon satellite. In this kind of experiment, the sea-level as measured by the altimeter is compared with the field observations, during an overflight of the area; the altitude of the satellite is measured by a laser station, located on the island, the sea-level is measured by coastal tide gauges (which can be accurately nivelated). In order to increase the number of observations, it is interesting to proceed to the calibration on short arcs, and therefore, the sea-level must be accurately determined under the track of the satellite, in a radius of about 25 km around the island. The expected precision for such altimetric measurements is some centimetres. The monitoring of the sea-level must be performed with this extreme accuracy, and this is possible only in an area where the sea level variability is small (Bongers and Wyrtki, 1987). The study presented in this paper is part of the works (Molines *et al.*, 1989 *a, b*) which were realised in order to estimate the sea level variability around Lampedusa Island. It was found that tidal effects were responsible of the major part of this variability (even if the tidal ranges are small in this part of the Mediterranean Sea) and therefore we had to perform a tidal modelisation for a better understanding and forecast of the tides there. The contribution of other effects such as meteorological effects, general circulation interference, meso-scale eddies propagating on the Tunisian shelf, fronts were also investigated and evaluated in the sea-level variability; the purpose of this paper is limited to tidal effects.

The Strait of Sicily is a dynamically very active area which communicates the Eastern and Western basins of the Mediterranean Sea and which can be schematically represented as a strongly stratified area, with Atlantic lighter water flowing eastward in the upper layer and more dense Levantine water flowing westward in the lower layer (Manzella *et al.*, 1988). The presence of these two water masses originates the principal oceanographic features of the area: frontal systems develops (*e.g.*, Grancini *et al.*, 1972), rings of atlantic water are observed on the Tunisian shelf, especially in winter months when the water exchange is maximum (Manzella *et al.*, 1990), strong internal waves are measured in the Strait of Sicily (Artale *et al.*, 1989). A rich literature is available for the oceanography of this region (a thorough review of this literature is given in Molines *et al.*, 1989 *a*).

Focusing our interest on tidal frequency motions, some studies can be briefly summarized: most of them are based on *in situ* observations, others use a mathematical approach.

In situ observations approach

• Concerning the sea level:

The tides of this basin can be represented with few harmonic constituents (Purga *et al.*, 1979), namely M_2 , S_2 , K_2 , N_2 , K_1 , O_1 , which are the only components greater than 1 cm.

The semidiurnal constituents have an amphidromic point slightly east of Pantelleria Island (Mosetti, 1987). It is noteworthy that these constituents show a great amplification on the African shelf. For example M_2 is about 52 cm at Gabes (Tunisia) and 42 cm at Sfax. The diurnal constituents are weak and uniform over the area with amplitude about 1.5 cm in the Eastern part and 3.2 cm inside the Sicily Channel. This information is completed on one hand by the data bank of the International Hydrographic Organization (1979; taking only into account the stations corresponding to records larger than one month), and on the other hand by four stations (Pantelleria, Lampedusa, Mazara del Vallo and an offshore gauge, referred as SG, 45 km North of Linosa where the local depth is 600 m) where bottom pressure measurements took place during the Janus experiment (Astraldi, *et al.* 1987). For these last stations, Manzella and colleagues kindly provided us the times series (six months) and we performed the harmonic analysis. The sites of interesting tide stations are shown in Figure 1. Some stations have been used to determine the forcing on open boundaries (Palermo, Cagliari, Cape Passero, Valetta and Tripoli), the others are used as control points for calibration purposes (La Goulette, Sfax, Gabes, Porto Empedocle, Mazara del Vallo, Marsala, Pantelleria, Lampedusa and SG).

• Concerning the currents in the tidal frequency band:

The kinetic energy in the tidal frequency band has been studied from current meter measurements, both in the Sicily Channel (between Cap Bon, Tunisia and Marsala, Sicily) and in a section from Sicily to Lybia, including the sicilian shelf around Malta (Grancini and Michelato, 1987). On the shelves, tidal currents represent most of the eddy kinetic energy (defined as $E_{\text{eddy}} = 1/2 (\sigma_u^2 + \sigma_v^2)$, where σ_u and σ_v represent the standard deviation of velocity components u and v); concerning the Sicily Channel the main characteristics are as follow:

- semidiurnal currents are almost of the same magnitude during the year and through the water column, corresponding to a barotropic tide;

- diurnal currents have a different behaviour: in general, on shelf areas, a maximum of variability is observed in the diurnal tidal band (stronger than in the semidiurnal band) and vary during the year and along the water column. Diurnal currents are stronger in summer than in winter (at some points they even completely disappear in winter) and they are stronger in the upper layer than in the lower layer, which is characteristic of a baroclinic motion.

- on the other hand, Artale *et al.* (1989) performed large-duration measurements of temperature profiles on the Adventure Bank, in the Tunisia-Sicily section. They found a very strong diurnal internal tide, probably produced by the flow over the edge of the shelf. The internal tide amplitude is estimated around 40 m, where the total water depth is about 100 m, and a pycnocline at roughly 40 m from the free surface. The occurrence of these internal waves pro-

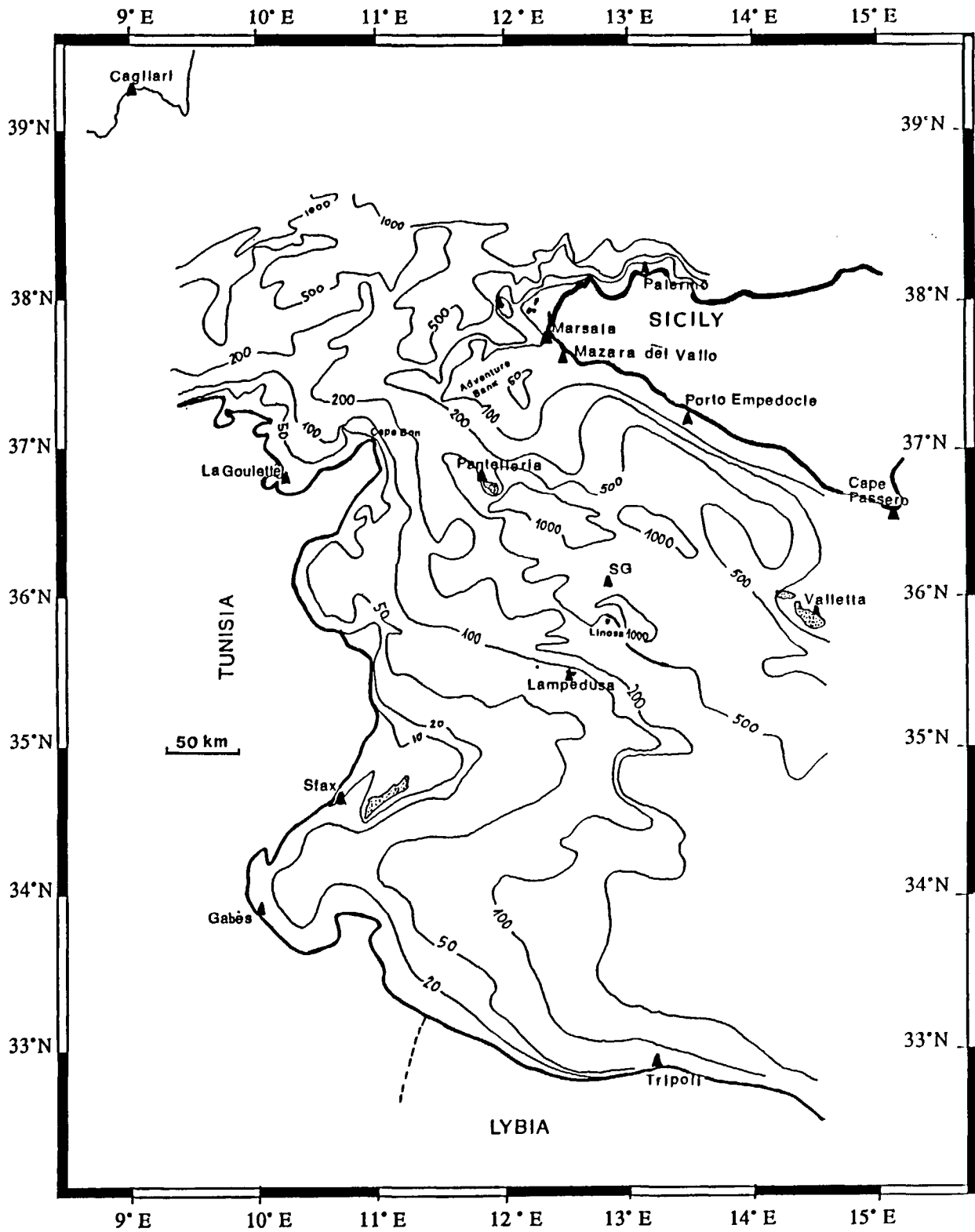


Figure 1

Sicily Strait and Tunisian shelf area. Tide gauge stations area indicated (▲). Depth are given in meters and limited to the modeled area.
 Carte du détroit de Sicile et du plateau continental tunisien. Les stations de mesure marégraphiques sont indiquées (▲). Les lignes isobathes sont cotées en mètres et limitées au domaine modélisé.

duces strong baroclinic diurnal currents. It seems a possible explanation for Grancini and Michelato's (1987) observations that diurnal currents are reinforced by baroclinic tide in summer conditions. Artale (1989), suggest that these internal waves are "tidally generated, topographically trapped baroclinic waves". These authors indicate that the semidiurnal internal waves are weak because of the proximity of the M_2 amphidromic point; this hypothesis is however questionable, as the forcing mechanism for internal waves comes from the velocities (which are strong in this area) instead of the elevation. In fact, following Baines (1982) the internal wave motion due to barotropic tides are driven by a body force F ,

$$F(z) = - (Q/\omega) N^2 z [h'(x)/h^2] \sin \omega t \mathbf{Z} \quad (1)$$

where Q is the barotropic flux vector (integrated velocity), N^2 is the local Brunt-Väissala frequency, ω the pulsation of the tidal motion, $h(x)$ is the bathymetric profile, here assumed as 2D for the sake of simplicity, \mathbf{Z} is the unit vector in the upward vertical direction. For a given density profile and topography, the driving force is proportional to Q/ω . Additional discussion on the generation of these internal waves will be done later in this paper.

Mathematical and numerical approach

In theoretical grounds, the tides of the Mediterranean Sea have been investigated in a global point of view by Defant (1961), giving the nodal locations in the Strait of Sicily. A numerical simulation of the M_2 tide was realized by Dressler (1980) for the whole Mediterranean; his model was forced by the tides at Gibraltar Strait and no other forcing was used. His results are therefore given in term of partial tide: nodal locations and Gulf of Gabes resonance are found in a qualitative point of view (amplitudes are too weak in the Gulf of Gabes). A spurious anti-amphidrome is found by Dressler (1980) in the vicinity of the amphidromic point, in the Strait of Sicily with a maximum amplitude of about 15 cm nearby Pantelleria Island, feature not observed in the nature.

The numerical study presented here is therefore the first realistic study realized for the Strait of Sicily and Tunisian shelf area. The study was formerly developed in the frame of the Topex/Poseidon calibration on Lampedusa, specially to check the sea surface slopes in the vicinity of the island. Additional interesting results concerning tidal dynamics for the area were found and are presented in this paper.

NUMERICAL MODEL

The model

The model is a finite difference 2D barotropic model. Detailed description is given in Le Provost and Fornerino

(1985). It uses a two-step predictor-corrector non-linear numerical scheme. The basic equations are:

- the non-linear momentum equation:

$$\partial \mathbf{U} / \partial t + \nabla \cdot (\mathbf{H}^{-1} \mathbf{U} \cdot \mathbf{U}) + \mathbf{f} \times \mathbf{U} = - \mathbf{g} \nabla z - 1/\rho (\tau_b) \quad (2)$$

-the continuity equation:

$$\partial \zeta / \partial t + \nabla \cdot \mathbf{U} = 0 \quad (3)$$

The symbols are:

$\mathbf{u} = u\mathbf{i} + v\mathbf{j}$: velocity vector

h : the water depth at rest

ζ : the sea level elevation above rest level

$H = h + \zeta$

$\mathbf{U} = \int \mathbf{u} dz$: depth-integrated velocity from $-h$ to ζ

f = Coriolis parameter

ρ = sea water density

τ_b : bottom friction stress taken as $\rho D/H^2 \mathbf{U} \cdot |\mathbf{U}|$, D is a drag coefficient. —

As the model is explicit, classical Courant Friedrich Levy (CFL) stability condition must be respected:

$$\Delta x / \Delta t > [\sqrt{2gh + u}]_{\max} \quad (4)$$

Δt is therefore determined from equation (3), when Δx , bathymetry and estimation of u are known. On the other hand, the corrector step uses centered derivatives which produce some unstabilities; a numerical horizontal viscosity is therefore introduced to balance this instability. The value of this numerical viscosity is theoretically estimated to $u^2 \Delta t / 2$; this estimation is used in the model. The numerical grid is a C-type staggered grid. On closed boundaries, the normal velocity is set to 0. On open boundaries, sea-level elevation ζ is prescribed and inferred from a tidal prediction with known constituents.

Mesh and boundary conditions

The model covers a $4.6^\circ \times 6^\circ$ area. The mesh (Fig. 2) was chosen with the following criteria:

- open boundaries are located away from amphidrome zone
- tidal constituents must be known on the open boundaries
- the model is westward bounded by the African shelf break.

The grid size is $\Delta x = \Delta y = 14.6$ km which gives a stable time step of $\Delta t = 80$ s. Bathymetry (deduced from nautical chart SHOM n° 9916) is characterized by shelf areas (Tunisian shelf, Adventure Bank) where depths are less than 100 m and much deeper central area where the maximum depth is nearly 1 700 m (Fig. 1). Note that the model does not include the shelf area around Malta.

Operation of the model

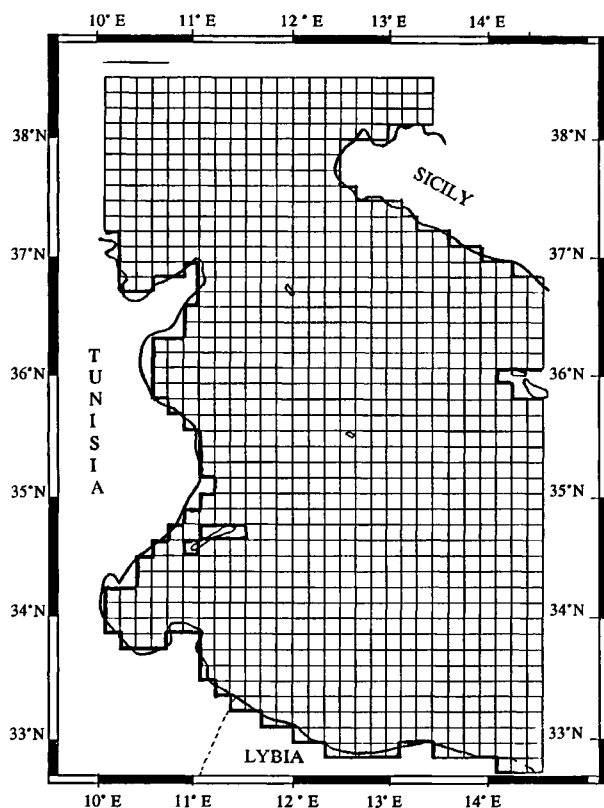


Figure 2

Mesh of the numerical model, $\Delta x = \Delta y = 14.6$ km.
Grille du modèle mathématique, $\Delta x = \Delta y = 14,6$ km.

The aim of this barotropic modelization is to produce results on the main tidal constituents. In this area, tidal amplitudes are rather small and we check on the data (as confirmed by Mosetti *et al.*, 1983) that non-linear constituents are less than 0.7 cm. For this reason, we assume that each constituent can be simulated separately, without taking into account the non-linear interactions: a run will be carried out for each constituent and open boundaries will be forced by the corresponding ζ . An *a posteriori* verification of this hypothesis is done checking the behaviour of M_4 and M_6 tides, derived from the non-linear propagation of the M_2 tide (Fig. 3). M_4 is generated by of the non-linear advective terms in the domain and M_6 is generated by the quadratic bottom friction (Le Provost, 1976). For these results, it is important to note that M_4 and M_6 amplitudes were clamped to 0 on open boundaries, so that amplitudes given on Figure 3 correspond only to the partial tides. M_4 have a maximum amplitude of 2.7 cm at Gabes with an amphidromic point situated in the Gulf of Gabes. M_6 have a maximum of 0.7 cm at Gabes too, with a complex pattern of three amphidromic points, indicated by (+) on Figure 3 b. From these results we conclude that non-linear effects are indeed very weak in the area, except in the inner Gulf of Gabes, where M_4 is emphasized by a standing wave effect.

Simulations are started from a rest condition and the

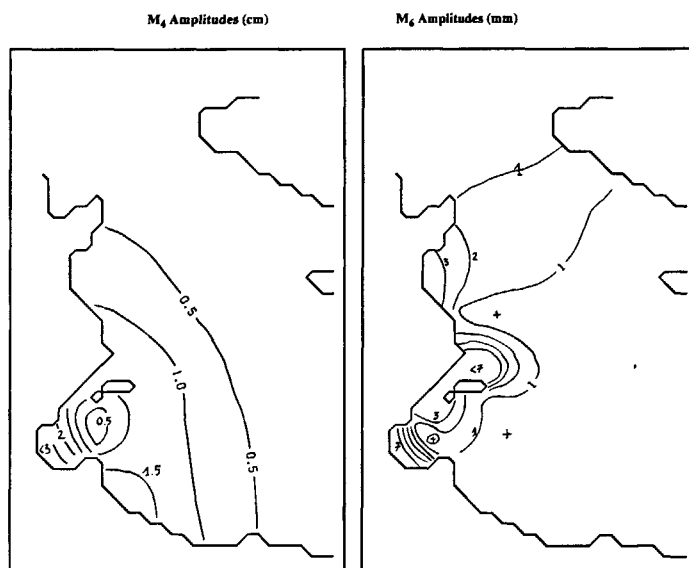


Figure 3

Co-range charts for M_4 (in cm) and M_6 (in mm) representing the non-linear effects produced by M_2 propagation in the model (partial tides). M_4 and M_6 were set to 0 on open boundaries.

Carte d'amplitude des ondes M_4 (en cm) et M_6 (en mm) indiquant le niveau des non-linéarités produites par la propagation de M_2 dans le modèle. M_4 et M_6 ont été imposées nulles sur les frontières ouvertes.

results are stored only when a steady state solution is reached (the steady state is reached when two successive tidal periods are almost identical everywhere in the model). When the model is run in a shallow water area (Le Provost and Fornerino, 1985; Molines *et al.*, 1989) typically five tidal periods are enough to obtain a steady state. In the case of this simulation, steady state is reached quickly in the northern part but up to twenty tidal periods are necessary for a complete stabilisation in the Gulf of Gabes and adjacent areas: this is probably due to the larger inertia of the deepest parts, which are practically non-dissipative.

TIDAL SIMULATIONS

SEMIDIURNAL CONSTITUENTS

M_2

Sea-level variations

M_2 was the first constituent to be simulated. Bottom friction was adjusted by a trial and error method in order to obtain the best fit for M_2 amplitudes and phases at the control points. The best value for the drag coefficient was found to be $D = 0.0021$, slightly smaller than the value (0.0025) commonly accepted. We check that the bottom

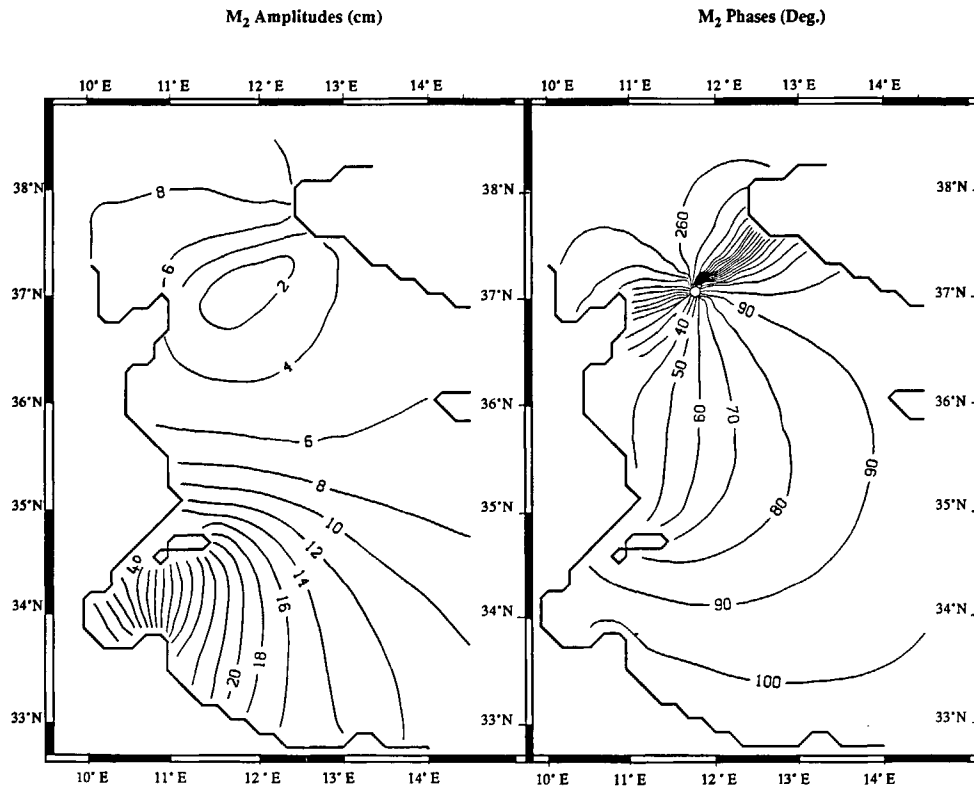


Figure 4

M₂ co-tidal and co-range charts. Phases (°) are related to local time (TU-1). Contour line increments are 2 cm for amplitudes and 10° for phases.
 Cartes cotidales de la marée M₂. Les phases (°) sont données par rapport aux heures locales (TU-1). Les lignes sont espacées de 2 cm pour les amplitudes et 10° pour les phases.

Table 1

Comparison of simulated and observed M₂ at nine control points.
 Comparaison observation-modèle pour l'onde M₂ en neuf points de contrôle.

Tide gauge	Amplitude (cm)		Phases (deg)	
	Obs	Model	Obs	Model
La Goulette	8.0	7.9	278	280
Sfax	41.6	42.5	105	92
Gabes	51.1	49.5	108	97
Marsala	6.8	6.8	235	238
Mazara del Vallo	4.3	4.5	190	197
Porto Empedocle	4.7	4.9	107	100
Lampedusa	6.6	6.5	74	74
Pantelleria	1.6	1.5	60	64
SG gauge	4.8	4.9	79	82

friction is only efficient on the shallow shelves and specially near the Tunisian coast and Gulf of Gabes. Cotidal and co-range maps are drawn on Figure 4. Comparison between the numerical results and observations are shown in Table 1. The agreement is quite good for the amplitudes with a RMS error of 0.6 cm. Phases are also in global good agreement (RMS error less than 10°). A strong resonance of the Gulf of Gabes is observed, in agreement with observations (IHO, 1979). The amphidromic point is located 20 km NW of Pantelleria Island. During the cali-

bration procedure, the drag coefficient was modified but the amphidrome remained at the same place, indicating that it corresponds to a strong feature.

Tidal currents

M₂ tidal currents have two regions of maximum values: in the Gulf of Gabes, due to the M₂ resonance, and on the Adventure Bank where both shallow waters and proximity of the amphidromic point enhance the tidal stream. Maximum values are about 0.15 m/s on the Adventure

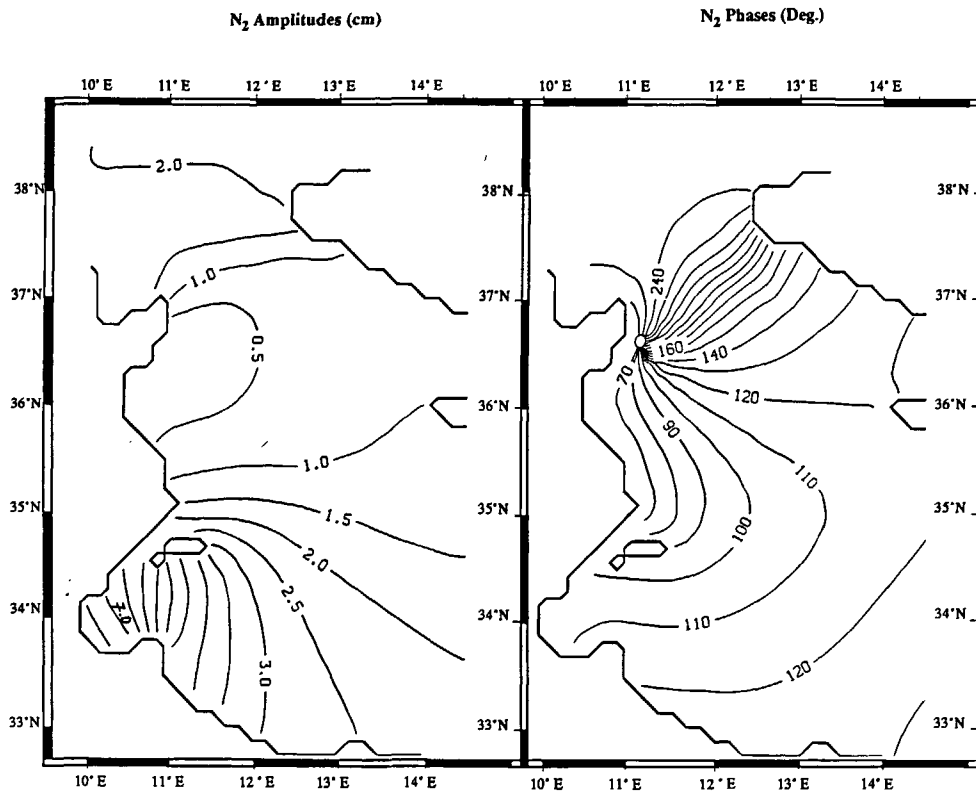


Figure 5

N_2 co-tidal and co-range charts. Phases ($^{\circ}$) are related to local time (TU-1). Contour line increments are 0.5 cm for amplitudes and 10° for phases.

Cartes cotidales de la marée N_2 . Les phases ($^{\circ}$) sont données par rapport aux heures locales (TU-1). Les lignes sont espacées de 0.5 cm pour les amplitudes et 10° pour les phases.

Table 2

Comparison of simulated and observed N_2 at nine control points.

Comparaison observation-modèle pour l'onde N_2 en neuf points de contrôle.

Tide gauge	Amplitude (cm)		Phases (deg)	
	Obs	Model	Obs	Model
La Goulette	2.0	1.8	250	255
Sfax	6.2	6.4	98	99
Gabes	8.8	7.7	107	107
Marsala	—	1.8	—	224
Mazara del Vallo	1.2	1.5	190	197
Porto Empedocle	0.9	1.0	127	132
Lampedusa	1.0	0.9	92	106
Pantelleria	0.3	0.5	172	172
SG gauge	0.7	0.8	96	121

Bank and about 0.30 m/s in the Gulf of Gabes. These values are relatively small but coherent with the small tidal range.

Unfortunately, Grancini and Michelato's (1987) paper does not give the values of tidal currents, information considered as confidential. However, they present time series which are absolutely coherent with these values on Adventure Bank.

N_2

Sea-level variations

No calibration was performed on the drag coefficient and we maintain the optimal value found for M_2 ($D = 0.0021$). Again, twenty tidal periods were used to spin up the model to a steady state; results are presented on Figure 5 and Table 2. There is still a good agreement with the observed data (RMS of 0.4 cm for amplitudes and 10° for phases). A noticeable phase discrepancy is observed at offshore tide gauge SG; no easy explanation can be given here. Comparing with M_2 , we note that the resonance of the Gulf of Gabes is much weaker and on the other hand, the ampli-

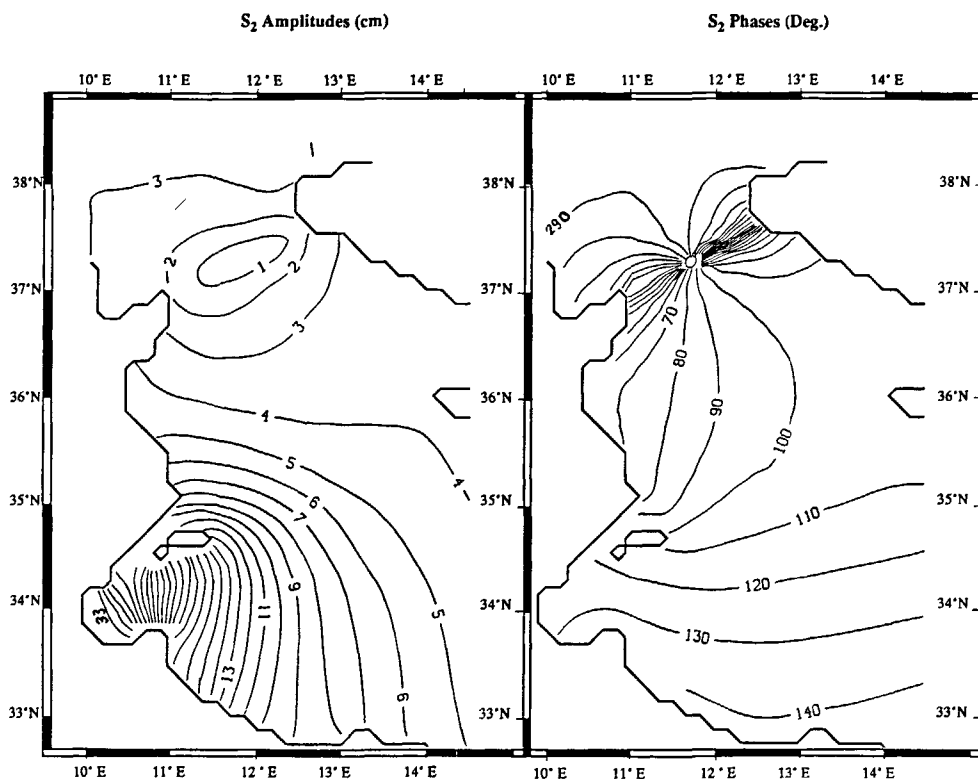


Figure 6

S₂ co-tidal and co-range charts. Phases (°) are related to local time (TU-1). Contour line increments are 1 cm for amplitudes and 10° for phases.

Cartes cotidales de la marée S₂. Les phases (°) sont données par rapport aux heures locales (TU-1). Les lignes sont espacées de 1 cm pour les amplitudes et 10° pour les phases.

Table 3

Comparison of simulated and observed S₂ at nine control points. Comparaison observation-modèle pour l'onde S₂ en neuf points de contrôle.

Tide gauge	Amplitude (cm)		Phases (deg)	
	Obs	Model	Obs	Model
La Goulette	3.0	2.9	305	310
Sfax	26.7	27.8	133	122
Gabes	36.4	34.6	137	129
Marsala	2.0	2.2	246	250
Mazara del Vallo	1.8	1.8	181	182
Porto Empedocle	3.3	3.5	105	107
Lampedusa	4.2	4.5	88	98
Pantelleria	1.9	2.2	72	88
SG gauge	3.1	3.6	87	99

dromic point is shifted westward, near the Tunisian coast, about 50 km South East of Cape Bon.

Tidal currents

N₂ tidal currents are very weak but their pattern are very similar to the M₂ tidal current pattern, with maximum values of 0.03 m/s on Adventure Bank and 0.03 m/s in the Gulf of Gabes.

S₂

Sea-level variations

S₂ results are shown on Figure 6 and Table 3. They were obtained following the same spin-up procedure. Amplitudes are almost correct (RMS of 0.7 cm) and also are the phases (RMS of 9°); the highest deviation occurs at Pantelleria (16°) which is near the amphidromic point. We note that the resonance of the Gulf of Gabes is even stonger (in term of input/output ratio) than the resonance, indicating that the free period of oscillation of the Gulf of Gabes is closer to S₂ period than M₂ period. The S₂ amphidromic point is slightly shifted to the North (about 20 km) in comparison with the M₂ amphi-

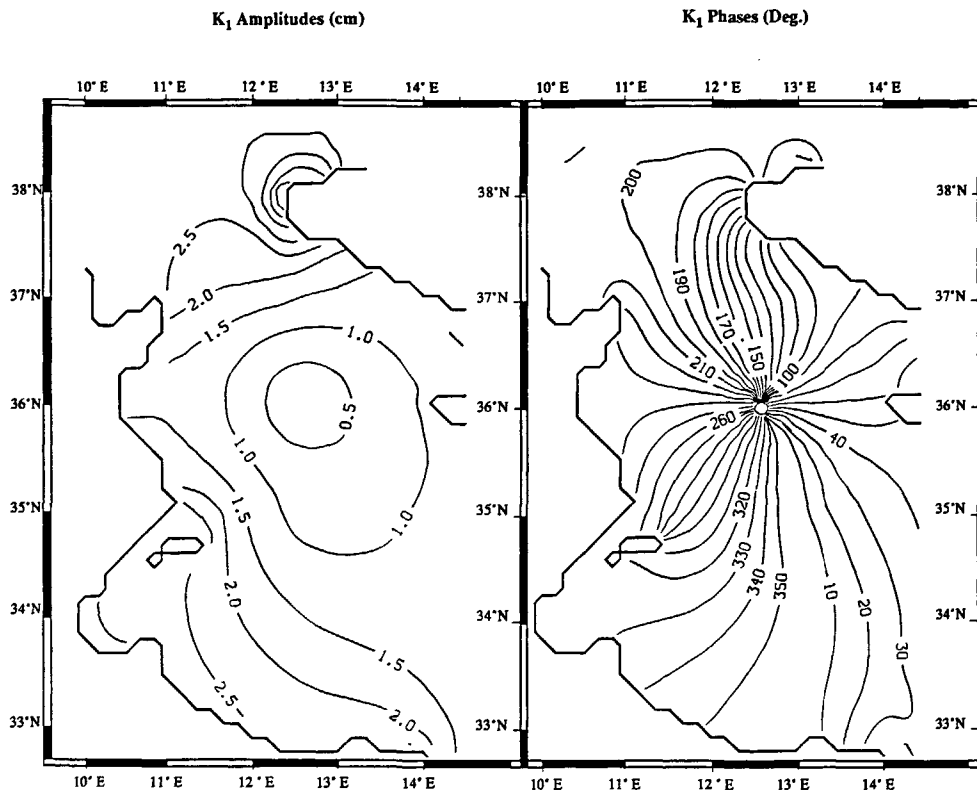


Figure 7

K_1 co-tidal and co-range charts. Phases ($^{\circ}$) are related to local time (TU-1). Contour line increments are 0.5 cm for amplitudes and 10° for phases.

Cartes cotidales de la marée K_1 . Les phases ($^{\circ}$) sont données par rapport aux heures locales (TU-1). Les lignes sont espacées de 0.5 cm pour les amplitudes et 10° pour les phases.

Table 4

Comparison of simulated and observed K_1 at nine control points.
Comparaison observation-modèle pour l'onde K_1 en neuf points de contrôle.

Tide gauge	Amplitude (cm)		Phases (deg)	
	Obs	Model	Obs	Model
La Goulette	3.0	3.0	211	207
Sfax	1.8	2.7	19	310
Gabes	2.5	3.1	4	325
Marsala	3.6	3.9	147	152
Mazara del Vallo	3.5	3.7	129	121
Porto Empedocle	1.8	1.4	107	90
Lampedusa	0.9	0.7	18	321
Pantelleria	2.0	1.5	187	187
SG gauge	0.5	0.3	93	95

dromic point; it lays just in the Sicily Channel, on the Cape Bon (Tunisia)-Marsala (Sicily) line.

Tidal currents

As for N_2 , the pattern is similar to the main semidiurnal M_2 . Maximum expected values are 0.07 m/s on Adventure Bank and 0.18 m/s in the Gulf of Gabes.

DIURNAL CONSTITUENTS

K_1

Sea-level variations

Results concerning K_1 are presented on Figure 7 and Table 4, obtained by a similar procedure than for semi-diurnal constituents. In particular, we still use a drag coefficient of $D = 0.0021$. Amplitude are everywhere weak, with a maximum of 5 cm near the western part of Sicily. This local maximum produces strong diurnal currents in the area, probably the signature of coastal trapped waves in this area, as suggested by the phase

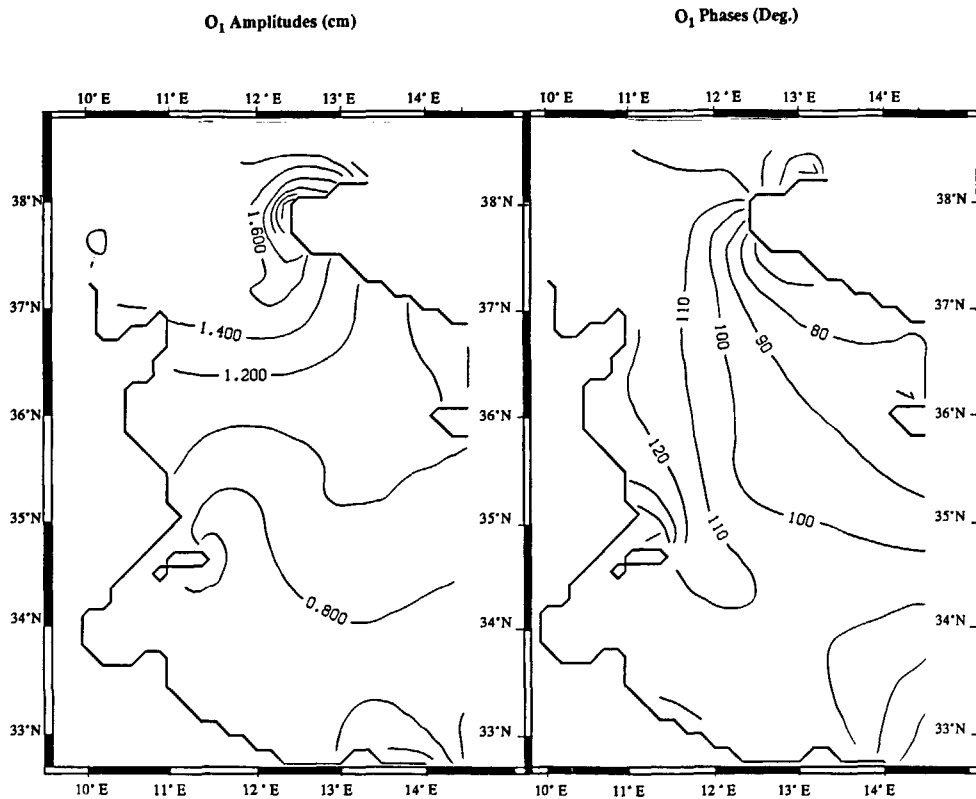


Figure 8

O₁ co-tidal and co-range charts. Phases (°) are related to local time (TU-1). Contour line increments are 0.2 cm for amplitudes and 10° for phases.

Cartes cotidales de la marée O₁. Les phases (°) sont données par rapport aux heures locales (TU-1). Les lignes sont espacées de 0.2 cm pour les amplitudes et 10° pour les phases.

Table 5

Comparison between observations and model results for O₁ constituent.
 Comparaison entre observations et résultat

Tide gauge	Amplitude (cm)		Phases (deg)	
	Obs	Model	Obs	Model
La Goulette	1.0	1.6	129	115
Sfax	0.8	0.6	96	115
Gabes	0.5	0.6	95	104
Marsala	1.8	2.2	108	88
Mazara del Vallo	1.6	2.1	88	67
Porto Empedocle	1.2	1.1	86	71
Lampedusa	0.7	0.9	—	95
Pantelleria	1.4	1.4	—	105
SG gauge	0.9	1.1	—	92

pattern around the Western extremity of Sicily. An amphidromic point is located nearby Linosa Island, very close to SG tide gauge. Phases are coherent but big discrepancies are observed in the Gulf of Gabes and Lampedusa. These differences may have various origins:

- local meteorological effects can corrupt the observations at S₁ frequency (Zetler, 1970) and therefore contaminate K₁ (for instance at Sfax S₁ is greater than K₁, International Hydrographic Organization, 1979);
- the linear distribution of amplitude and phases along the

Malta-Lybia line was chosen for the sake of simplicity and also for the lack of off shore observations; this repartition is perhaps not adequate;

- in the model we deal with barotropic tides. In fact we have seen (Artale *et al.*, 1989) that strong internal diurnal tides are observed at least on Adventure Bank. A part of the barotropic energy is thus converted into the baroclinic mode and locally dissipated.

Tidal currents

As for M₂, tidal currents are maximum over the Adventure

Bank. In the Gulf of Gabes they are not particularly stronger than anywhere else. The maximum values (about 0.25 m/s) are stronger than for M_2 currents. The dominance of the diurnal currents on the Adventure Bank was one of the characteristic features mentioned by Grancini and Michelato (1987). It is produced by the local maximum of K_1 elevation that we already mentioned; such strong diurnal currents flowing above a continental shelf break are able to generate internal waves (Baines, 1982; Hibiya, 1983). As indicated in equation 1, the internal wave driving force F_w is proportional to Q/w for a given topography and stratification. Considering the maximum values of the tidal currents, we deduce that $F_{K1} \approx 4 F_{M2}$ and even $F_{O1} \approx F_{M2}$ (see below). This is an explanation for the diurnal character of the internal waves in this area. However, as pointed out by Artale *et al.* (1989), diurnal frequencies are sub-inertial at this latitude and the observed diurnal internal waves must be topographically trapped. This is a reason for their local character.

O_1

O_1 is very weak and therefore boundary conditions are not particularly reliable. However we present the results for O_1 as they confirm the trapping of energy around the Western extremity of Sicily with maximum value ≈ 2 cm

Acknowledgements

During this job, many contacts were taken with Italian Researchers and I particularly acknowledge the help of Dr. Manzella and his team, which provide us sea level

(Fig. 8). This is the most interesting feature concerning diurnal tides. Processes of topographic trapping of energy greatly depends on the slope of the bottom topography. The actual grid size of the model (14.5 km) is far too coarse for a correct resolution of this problem, so that these results are to be considered as diagnostic only. O_1 tidal currents are consequently emphasized on the Adventure Bank (maximum of 0.07 m/s), comparable to the S_2 currents.

SUMMARY AND CONCLUSIONS

The main tidal constituents have been modeled for the Strait of Sicily and Tunisian shelf area.

Our numerical results are in good agreement with field observations, mainly for semidiurnal (the tuning of the model was realized for the M_2 wave, and improvement for the diurnal constituent may be probably obtained by refining the tuning for these constituents). Position of amphidromic points has also been clarified. Tidal ranges are small but tidal currents are predominant in the shallow waters of Adventure Bank and Gulf of Gabes.

These results suggest that the complex stratification and

REFERENCES

- Artale V., A. Provenzale and R. Santoleri (1989). Analysis of internal temperature oscillations of tidal period on the Sicilian continental shelf. *Contin. Shelf Res.*, **9**, 10, 867-888.
- Astraldi M., C. Galli, G.P. Gasparini, E. Lazzone and G.M.R. Manzella (1987): The Janus experiment. Internal Report, TR 140, CNR/CREA, La Spezia, 38 pp.
- Baines P.G. (1982). On Internal Tide Generation Models. *Deep-Sea Res.*, **29**, 3A, 307-338.
- Bongers T. and K. Wyrski (1987). Sea Level at Tahiti. A Minimum of Variability. *J. phys. Oceanogr.*, **17**, 1, 164-168.
- Defant A. (1961). *Physical Oceanography*. Pergamon Press, Oxford, Vol. 2, 598 pp.
- Dressler R. (1980). Hydrodynamisch-numerische untersuchungen der M_2 . Gezeit und einiger Tsunamis im Europäischen Mittelmeer. Mitteilungen des Instituts für Meereskunde der Universität Hamburg, n° XXIII, 1-30.
- Grancini G.P., A. Lavenia and F. Masetti (1972). A contribution to the hydrology of the Strait of Sicily. *Proceedings Saclant Conference*, **7**, 68-81.
- Grancini G.P. and A. Michelato (1987). Current Structure and Variability in the Strait of Sicily and Adjacent Area. *Annls Geophys.*, **5B**, 1, 75-88.
- Hibiya T. (1986). Generation Mechanism of Internal Waves by Tidal Flow Over a Sill. *J. geophys. Res.*, **91**, C6, 7697-7708.
- International Hydrographic Organization (1979). IHO Tidal constituent Bank. Ottawa, 93 pp.
- Le Provost C. (1976). Theoretical analysis of the structure of the tidal wave's spectrum in shallow water area. *Mémoire de la Société Royale des Sciences de Liège, 6^{ème} série, tome X*, 97-111.
- Le Provost C. and M. Fornerino (1985). Tidal Spectroscopy of the English Channel with a Numerical Model. *J. phys. Oceanogr.*, **15**, 8, 1009-1031.
- Manzella G.M.R., G. P. Gasparini and M. Astraldi (1988). Water exchanges between the eastern and western Mediterranean through the Strait of Sicily. *Deep-Sea Res.*, **35**, 1021-1035.
- Manzella G.M.R., T.S. Hopkins, P.J. Minett and E. Nacini (1990). Atlantic water in the Strait of Sicily. *J. geophys. Res.*, **95**, C2, 1569-1576.
- Molines J.-M., M. Fornerino and C. Le Provost (1989). Tidal spectroscopy of a coastal area: observed and simulated tides of the Lake Maracaibo system. *Contin. Shelf Res.*, **9**, 4, 301-323.
- Molines J.-M., L. Monsaingeon and C. Le Provost (1989 a). Topex/Poseidon calibration plan: Sea level variability induced by geophysical environmental parameters in the area of the nominal site of Lampedusa. A bibliographical survey. Contract report CNES/SBS D2921, 42 pp.
- Molines J.-M., L. Monsaingeon and C. Le Provost (1989 b). Topex/Poseidon calibration plan. Part II: Numerical modelling and

optimal instrumentation of the site. Contract report CNES/SBS D3380, 31 pp.

Mosetti F. (1987). Distribuzione delle maree nei mari Italiani. *Boll. Oceanol. teor. appl.*, **5**, 1, 65-72.

Mosetti R., F. Mosetti and N. Purga (1983). On Some Short Period Tides in the Seas Around Italy. *Boll. Oceanol. teor. appl.*, **1**, 1, 49-66.

Purga N., F. Mosetti and E. Accerboni (1979). Tidal Harmonic Constants for Some Mediterranean Harbours. *Boll. Geofis. teor. appl.*, **21**, 81, 72-81.

Zetler B. (1970). Radiational Ocean Tides along the Coast of United States. *J. phys. Oceanogr.*, **B**, 34-38.
